Available online at www.sciencedirect.com
SCIENCE DIRECT®
Journal of Chromatography A, 991 (2003) 31–45
JOURNAL OF CHROMATOGRAPHY A
www.elsevier.com/locate/chroma

# Theoretical and experimental study of binary perturbation peaks with focus on peculiar retention behaviour and vanishing peaks in chiral liquid chromatography ☆

Patrik Forssén[a], Johan Lindholm[b], Torgny Fornstedt[b,*]

[a]*Department of Information Technology/Scient. Comp., Uppsala University, Box 337, SE-751 05 Uppsala, Sweden*
[b]*Center for Surface Biotechnology, BMC, Box 577, SE-751 23 Uppsala, Sweden*

Received 26 October 2002; received in revised form 14 January 2003; accepted 22 January 2003

**Abstract**

The perturbation peak theory was recently developed for acquiring binary isotherm data using the perturbation method (PM) and it was applied for some chiral systems. However, the binary plateaus of these systems were only weakly to moderately nonlinear. In this article the perturbation theory for LC, is developed for both retention times and peak areas and is verified by systematic experiments over the whole range of non-linearity. Attention is focused on non-linear effects that complicate the proper use of the PM method under moderately to strongly non-linear conditions. A serious complication was that the second perturbation peak vanished already at moderate plateau concentrations. A solution to this problem based on a firm theoretical basis and verified experimentally is presented. We also investigated a peculiar retention dependence on the binary plateau concentration, as the retentions of the two perturbation peaks of the binary plateau was compared with the single plateau peak of the more retained enantiomer.


*Keywords:* Perturbation method; Adsorption isotherms; Enantiomer separation; Retention behaviour

## 1. Introduction

The current trend in preparative chiral liquid chromatography (LC) is towards more complex and continuous adsorption-based processes such as recycling [1] and simulated moving bed [2,3]. This has made computer simulations an increasingly important optimisation tool today. However, the proper use of computer simulations requires a priori determination of the fundamental thermodynamics [4,5]. In chiral separations at least two components are to be separated and their isotherms are not independent, but competitive. Thus, knowledge of the competitive adsorption isotherms is the main prerequisite for proper modelling of chiral LC.

The traditional frontal analysis (FA) invented by Tiselius [6] is today considered to be the most accurate method for measuring a single-component isotherm [5]. Jacobson et al. presented a practical approach, firmly supported by theory, to acquire

☆Presented at the 15th International Symposium on Preparative and Process Chromatography, Washington, DC, 16–19 June 2002.

*Corresponding author. Fax: +46-18-555-016.
*E-mail address:* torgny.fornstedt@ytbioteknik.uu.se (T. Fornstedt).

0021-9673/03/$ – see front matter 
doi:10.1016/S0021-9673(03)00213-9

competitive isotherms in two-component high-performance liquid chromatography (HPLC) systems [7]. However, the method is time-consuming and tedious, especially for the competitive case requiring fractionations for proper quantification of the intermediate plateau levels.

Although the perturbation peak (PM) method was introduced 40 years ago [8,9] to measure single component isotherms it has seldom been used in LC. A disadvantage compared to the FA method is that the relative areas of the perturbation peaks must be measured in order to determine an experimental isotherm [10], and this has not been done for LC yet. Recently, Seidel-Morgenstern and co-workers [11,12] and Jandera et al. [13] have used the PM method for the first time in the competitive mode. The PM method utilizes the principle that the retention time of a perturbation peak depends on the partial derivatives of the isotherm at the plateau concentration. The perturbation peaks are created by disturbing the established equilibrium in the system with an injection of either small excesses or deficiencies of the components. The perturbation theory for peak retention times, but not for peak areas, has been summarised for LC by Blümel et al. [12]. It should also be mentioned that the PM method in the binary mode was used only for weakly to moderately non-linear systems and not for heterogeneous adsorption models [11–13].

The aim of this study was to investigate important non-linear effects when applying the PM method for racemic mixtures in LC under moderately and strongly non-linear conditions. Under these conditions the use of the PM method was hindered because of a recently reported phenomenon; namely, that the second perturbation peak on a racemic plateau vanished during moderate to strong non-linearity [14]. This is an especial serious problem when using immobilised proteins [15] as chiral stationary phases showing heterogeneous adsorption characteristics and which require concentration ranges where at least one of the sites is overloaded [16,17]. If an adequate concentration range is not used the wrong adsorption model might fit better, which was recently demonstrated [18]. The theory of vanishing perturbation peaks has recently been explained in a ''not easy way'' for gas chromatography (GC) [19], but not for chiral LC. The aim of the actual study is threefold:

(1) To present a complete theory for binary perturbation peaks in (chiral) LC including both retention times and peak areas.

(2) To investigate, both theoretically and experimentally, a solution to the problem of vanishing perturbation peaks on a racemic plateau.

(3) To investigate, both theoretically and experimentally, a ''peculiar'' retention behaviour, as the binary peaks are compared with the single plateau peaks of respective component.

## 2. Theory

### 2.1. Retention time and area of perturbation peaks

In this section expressions both for the retention time and for the areas of perturbation peaks in liquid chromatography will be derived. The case of gas chromatography has been covered elsewhere [10], but differs from the case of LC because of the compressibility of gases, a different injection technique and work with mole fractions rather than concentrations. General expressions for the situation with any number of components can be derived, however here a two-component situation as assumed, i.e., at most two components dissolved in an inert carrier fluid, both in the mobile phase and in the sample. Experimentally it is assumed that a small sample is injected into the mobile phase and that this will give rise to two small peaks, known as system peaks or perturbation peaks.

First the basic assumption is made that the moment of order zero (peak area) and the normalised moment of order one (mean peak retention time) of the column response are independent of kinetics and dispersion. The chromatographic process in the case of perturbation peaks can then be described by a system of two coupled partial differential equations, one for each component:

$$\begin{cases} \dfrac{\partial c_i(x,t)}{\partial t} + F \cdot \dfrac{\partial q_i[c_1(x,t), c_2(x,t)]}{\partial t} + u \cdot \dfrac{\partial c_i(x,t)}{\partial x} = 0, \quad 0 \le x \le L, \quad t \ge 0, \quad i = 1, 2 \\ c_i(x,0) = c_{0,i} \\ c_i(0,t) = a_i \cdot \delta(t-0) \end{cases} \tag{1}$$

where $x$ is distance along the column, $t$ is time, $c_i$ is the concentration in the mobile phase, $q_i$ is the concentration in the stationary phase given as func-

tions of the concentrations $c_1, c_2$ in the mobile phase (the isotherm function), $c_{0,i}$ is the initial mobile phase concentration (plateau), $\delta(t-0)$ is a unit Dirac distribution centred at time zero and $a_i$ is the amplitude of the injection. There are also the following constants: $F$ is the phase ratio, $L$ is the column length and $u$ is the linear velocity of the mobile phase. It is reasonable to assume that the linear velocity $u$ is constant, because we consider liquid chromatography with incompressible fluids under nearly isothermal conditions.

Assuming small perturbations (injections) the solution to Eq. (1) can be derived. We will not go through all the steps in the solution; they are similar to those in Ref. [10], but only write down the resulting expressions. Let the matrix **M** be:

$$\mathbf{M} = \begin{pmatrix} m_{1,1} & m_{1,2} \\ m_{2,1} & m_{2,2} \end{pmatrix} = \begin{pmatrix} 1 + F \cdot \dfrac{\partial q_1}{\partial c_1} & F \cdot \dfrac{\partial q_1}{\partial c_2} \\ F \cdot \dfrac{\partial q_2}{\partial c_1} & 1 + F \cdot \dfrac{\partial q_2}{\partial c_2} \end{pmatrix} \Bigg|_{c_1 = c_{0,1}, c_2 = c_{0,2}} \quad (2)$$

where the partial derivatives $\partial q_1/\partial c_1, \partial q_1/\partial c_2, \partial q_2/\partial c_1, \partial q_2/\partial c_2$of the isotherm functions $q_1, q_2$ are evaluated at the initial mobile phase concentrations $c_{0,1}$, $c_{0,2}$. The partial derivatives can be estimated numerically or, if one have closed expressions for the isotherm functions, by symbolic differentiation. E.g., for a competitive Langmuir type isotherm, then:

$$q_i = \frac{a_i c_i}{1 + b_1 c_1 + b_2 c_2} \quad (3)$$

where $i = 1, 2$ and $a_i$, $b_i \geq 0$, and:

$$\begin{aligned} \frac{\partial q_1}{\partial c_1} &= \frac{a_1(1 + b_2 c_2)}{(1 + b_1 c_1 + b_2 c_2)^2}, \\ \frac{\partial q_1}{\partial c_2} &= -\frac{a_1 b_2 c_1}{(1 + b_1 c_1 + b_2 c_2)^2}, \\ \frac{\partial q_2}{\partial c_1} &= -\frac{a_2 b_1 c_1}{(1 + b_1 c_1 + b_2 c_2)^2}, \\ \frac{\partial q_2}{\partial c_2} &= \frac{a_1(1 + b_2 c_2)}{(1 + b_1 c_1 + b_2 c_2)^2} \end{aligned} \quad (4)$$

In order to determine the peak areas we also need the matrix **P**:

$$\mathbf{P} = \begin{pmatrix} p_{1,1} & p_{1,2} \\ p_{2,1} & p_{2,2} \end{pmatrix} = \begin{pmatrix} \dfrac{(m_{1,1} - m_{2,2}) + D}{2m_{2,1}} & \dfrac{(m_{1,1} - m_{2,2}) - D}{2m_{2,1}} \\ 1 & 1 \end{pmatrix} \quad (5)$$

where $D = \sqrt{(m_{1,1} - m_{2,2})^2 + 4m_{1,2}m_{2,1}}$ and its inverse $\mathbf{P}^{-1}$:

$$\mathbf{P}^{-1} = \begin{pmatrix} p_{1,1}^{-1} & p_{1,2}^{-1} \\ p_{2,1}^{-1} & p_{2,2}^{-1} \end{pmatrix} = \begin{pmatrix} \dfrac{m_{2,1}}{D} & -\dfrac{(m_{1,1} - m_{2,2}) - D}{2D} \\ -\dfrac{m_{2,1}}{D} & \dfrac{(m_{1,1} - m_{2,2}) + D}{2D} \end{pmatrix} \quad (6)$$

Finally, define $\bar{a}_i$ as:

$$\bar{a}_i = (c_{s,i} - c_{0,i}) t_{inj} = (c_{s,i} - c_{0,i}) \cdot \frac{V_{inj}}{F_m}$$

where $i = 1, 2$ (7)

where $c_{s,i}$ is the sample concentrations, $V_{inj}$ is the injected volume, $F_m$ is the mobile phase flow and $t_{inj} = V_{inj}/F_m$ is the injection time.

The individual response of component $i$ will now be two peaks located at the mean retention times $t_{R,1}$ and $t_{R,2}$ where:

$$\begin{aligned} t_{R,1} &= t_0 \cdot \frac{(m_{1,1} + m_{2,2}) + D}{2}, \\ t_{R,2} &= t_0 \cdot \frac{(m_{1,1} + m_{2,2}) - D}{2}, \end{aligned} \quad (8)$$

where $t_0$ is the column hold-up time. Here it is worth noticing that the perturbation peaks will have the same mean retention time for both components, this is also known as the ''coherence condition''. This expression is actually misleading in this case; it is not a condition that is needed to solve Eq. (1) but rather a result one gets after solving it. That is, we have that Eq. (1)⇒Eq. (8)⇒''coherence'', not, as is stated in, e.g., Ref. [12], that Eq. (1)+''coherence''⇒Eq. (8). The corresponding area $\psi_{ij}$ of the $j$th perturbation peak in component $i$ will be:

$$\psi_{ij} = p_{ij}\left(p_{j1}^{-1}\bar{a}_1 + p_{j2}^{-1}\bar{a}_2\right) \quad (9)$$

where the area $\psi_{ij}$ can be positive or negative.

In practice, it is not possible, in general, to detect

the individual peaks of the separate components, but only the sum of all peaks of all components. Assuming linear detector response, with detector response factor $f_i$ for component $i$, we have that the mean retention time $t_{R,j}$ of peak number $j$ is as in Eq. (8) and that the total area $\psi_j$ is:

$$\psi_j = (f_1 p_{1j} + f_2 p_{2j}) \cdot (p_{j1}^{-1} \bar{a}_1 + p_{j2}^{-1} \bar{a}_2) \quad (10)$$

Although the number of perturbation peaks will be the same as the number of components in the sample, it is not possible to attribute a peak to an individual component. This is because a peak represents the response to a perturbation of the concentrations of all sample components.

### 2.2. Numerical verification of the theory

In order to verify the expressions in Eqs. (8) and (10), we approximate the boundary conditions (injection profile) in Eq. (1) by:

$$c_i(0,t) = \begin{cases} c_{s,i} & \text{for} \quad t \le t_{inj} \\ 0 \text{ otherwise} \end{cases} \quad (11)$$

Now the solution of Eq. (1) can be approximated numerically by using a finite difference method [4] where we also take into account the dispersion described by the number of theoretical plates $N$. The solution for a two-component case is shown in Table 1, were it is also compared with the results of Eqs. (8) and (10) and an excellent agreement was observed. All simulated chromatograms in the figures were calculated using the finite difference method.

Table 1
Comparison between mean retention times $t_R$ and peak areas $\psi$ calculated in two different ways

| | Theoretical | | Numerical | |
|---|---|---|---|---|
| | $t_R$ (min) | $\psi$ | $t_R$ (min) | $\psi$ |
| Fast peak | 4.0086 | $-1.1206 \cdot 10^{-7}$ | 4.0171 | $-1.1206 \cdot 10^{-7}$ |
| Slow peak | 5.1914 | $5.021 \cdot 10^{-8}$ | 5.1939 | $5.021 \cdot 10^{-8}$ |

The theoretical calculations uses Eqs. (8) and (10) and the numerical calculations uses a finite difference approximation of Eqs. (1) and (11). The injection was 5 μl of a sample with concentrations $c_{s,1} = 0.03$ *M*, $c_{s,2} = 0.06$ *M* on a binary plateau with concentrations $c_{0,1} = 0.05$ *M*, $c_{0,2} = 0.05$ *M*. All other parameters are the same as for system II, Table 2.

### 2.3. Vanishing peaks and optimal injections

It has been noted that under some conditions, a perturbation peaks can vanish, i.e., the total area $\psi_j$ becomes zero, which is a drawback of the perturbation peak method for determining of isotherms. In this section it will be described how to calculate under what conditions this may happen, i.e., determine what injections at the column inlet causes one or more perturbation peaks to vanish at the column outlet. As will be demonstrated, there is always possible to get clearly detectable perturbation peaks. Nevertheless, the conditions where perturbation peaks vanish is also very useful, e.g., they can be used to determine isotherm parameters [19], or verify the correctness of isotherm parameters determined in another way.

Assuming that rank $(\mathbf{P}) = 2$ in Eq. (5) and $\Sigma_{i=1}^{2} f_i p_{ij} \neq 0$, it is easy to show that any injection concentration $c_{s,i}$ can be written as:

$$c_{s,i} = c_{0,i} + \beta_1 p_{i1} + \beta_2 p_{i2} \quad (12)$$

where $\beta_k$ is a constant. It is also possible to show that if $\beta_k$ is 0 this will result in the vanishing of the perturbation peak with mean retention time $t_{R,k}$. Geometrically this means that for a fixed mobile phase concentration there are two lines, one for $\beta_1 = 0$ and one for $\beta_2 = 0$, in the sample composition space that indicate the sample compositions for which one of the two perturbation peaks will vanish, see Fig. 4a.

Though a vanishing perturbation peaks may yield useful information, it is very often desirable to have clearly detectable perturbation peaks, e.g., to measure retention times in order to determine isotherm parameters. Therefore, in this study we describe how to calculate ''optimal'' injections, i.e., sample compositions that will give two perturbation peaks with the same area, and under all degrees of non-linear conditions. Assuming equal response factor it is possible to show that any injection with the following concentrations:

$$c_{s,1} = c_{0,1} - \mu, \quad c_{s,2} = c_{0,2} + \mu \quad (13)$$

for some number $\mu$ (positive or negative), chosen so that $c_{s,1} \ge 0$ and $c_{s,2} \ge 0$, will always yield two perturbation peaks with the same area but opposite

signs, i.e., one positive and the other one negative. Notice that this optimal injection does not depend on the isotherm. The optimal injection in the case where both peaks have the same sign can be written:

$$c_{s,1} = c_{0,1} + \mu\left(\frac{a^2 - b^2 + a}{a+1}\right),$$
$$\text{where} \quad a = \frac{m_{1,1} - m_{2,2}}{2m_{2,1}}, b = \frac{D}{2m_{2,1}};$$
$$c_{s,2} = c_{0,2} + \mu \tag{14}$$

for some number $\mu$ (positive or negative), chosen so that $c_{s,1} \geq 0$ and $c_{s,2} \geq 0$. These expressions are less useful in practice because they depend on the isotherm. Geometrically Eqs. (13) and (14) mean that for a fixed mobile phase concentration there are two lines in the sample composition space that indicate the sample compositions where one will get optimal injections. Along one line we will get two perturbation peaks with the opposite sign and along the other line we will get two perturbation peaks with the same sign, see Fig. 4a.

*2.3.1. Proof of Eqs. (13) and (14)*

The condition that the perturbation peaks have the same area is $|\psi_1| = |\psi_2|$ (remember that the peak area might be negative) this can also be written:

$$\psi_1 - s\psi_2 = 0, \quad \text{where}$$
$$s = \begin{cases} 1, & \text{if the peaks have the same sign} \\ -1, & \text{if the peaks have opposite sign} \end{cases} \tag{15}$$

According to Eq. (10):

$$\psi_j = \gamma_j\left(p_{j1}^{-1}\bar{a}_1 + p_{j2}^{-1}\bar{a}_2\right) \tag{16}$$

where $\gamma_j = \Sigma_{i=1}^{2} f_i p_{ij}$.

The condition Eq. (15) can be written in matrix–vector notation as:

$$\left(\gamma_1 \mathbf{p}_1^{-1} - s\gamma_2 \mathbf{p}_2^{-1}\right) \cdot \begin{pmatrix} \bar{a}_1 \\ \bar{a}_2 \end{pmatrix} = \mathbf{N}\bar{\mathbf{a}} = 0 \tag{17}$$

where $\mathbf{p}_i^{-1}$ is row number $i$ of $\mathbf{P}^{-1}$. From this we see that an optimal injection must have $\bar{\mathbf{a}} \in N(\mathbf{N})$, i.e., $\bar{\mathbf{a}}$ belonging to the nullspace, or kernel, of $\mathbf{N}$ for which a basis matrix $\mathbf{N}_0$ can be calculated. If rank($\mathbf{P}$) = 2 then the dimension of $N(\mathbf{N})$ is 1, i.e., a line, and $\mathbf{N}_0$ is a vector. Using Eq. (7) an optimal injection can be written:

$$\bar{\mathbf{a}} = (\mathbf{c}_s - \mathbf{c}_0)t_{inj} \in N(\mathbf{N}) \Leftrightarrow \mathbf{c}_s = \mathbf{c}_0 + \mu\mathbf{N}_0 \tag{18}$$

where $\mathbf{c}_s = (c_{s,1}, c_{s,2})^T$, $\mathbf{c}_0 = (c_{0,1}, c_{0,2})^T$ and $\mu$ is any number chosen so that $c_{s,1} \geq 0$ and $c_{s,2} \geq 0$.

According to Eqs. (5) and (6) the matrix $\mathbf{P}$ and its inverse $\mathbf{P}^{-1}$ can be written:

$$\mathbf{P} = \begin{pmatrix} a+b & a-b \\ 1 & 1 \end{pmatrix}, \mathbf{P}^{-1} = \begin{pmatrix} \frac{1}{2b} & -\frac{a-b}{2b} \\ -\frac{1}{2b} & \frac{a+b}{2b} \end{pmatrix} \tag{19}$$

where $a$ and $b$ are as in Eq. (14). Using Eq. (16) we have that:

$$\gamma_1 = f_1(a+b) + f_2, \quad \gamma_2 = f_1(a-b) + f_2 \tag{20}$$

Inserting Eqs. (19) and (20) into Eq. (17) with $s = -1$, i.e., peaks with opposite sign, one gets that:

$$\mathbf{N} = \left(\frac{f_1(a+b)+f_2}{2b} - \frac{f_1(a-b)+f_2}{2b}, - \frac{[f_1(a+b)+f_2](a-b)}{2b} + \frac{[f_1(a-b)+f_2](a+b)}{2b}\right) = (f_1, f_2) \tag{21}$$

and then $\mathbf{N}_0 = (-f_2/f_1, 1)^T$. Assuming that $f_1 = f_2$ and inserting $\mathbf{N}_0$ into Eq. (18) one gets Eq. (13).

In the same way one can prove that for $s = 1$, i.e., peaks with the same sign:

$$\mathbf{N}_0 = \left(\frac{f_1(a^2 - b^2) + f_2 a}{f_1 a + f_2}, 1\right)^T \tag{22}$$

Assuming that $f_1 = f_2$ and inserting $\mathbf{N}_0$ into Eq. (18) one gets Eq. (14).

## 3. Experimental

### *3.1. Apparatus*

All HPLC experiments were performed with a Hewlett-Packard HP 1100 Chemstation with an autoinjector, equipped with a valve-switching unit with total 10-port valves, a built in diode-array UV detector, two pumps and a working station personal computer (Agilent Technologies, Palo Alto, CA, USA). The mixer, Agilent 1100 (60×4.6 mm I.D.)

were bypassed by a short 0.17 mm polyether ether ketone (PEEK) capillary. All connections from the system were short sections of 0.17 mm PEEK capillaries. The columns were placed in a water jacket and its temperature was kept constant using a MN6 Lauda circulating water-bath (Lauda, Königshofen, Germany). The pH was measured with a Metrohm 632 pH meter (Metrohm, Herisau, Switzerland).

### 3.2. Chemicals

4-Androsten-3,17-dione (AD) and 11α-hydroxyprogesterone (11α-OH-PS) of minimum 98% purity were obtained from Sigma (Stockholm, Sweden). (+)-Methyl-L-mandelate (LM) and (−)-methyl-D-mandelate (DM) (purity>99%) were obtained from Fluka (Buchs, Switzerland). The acetate buffers were prepared from acetic acid (purity>99.8%) from Riedel-de Haën (Seelze, Germany) and anhydrous sodium acetate (purity>99%) and 2-propanol LiChrosolv from Merck (Darmstadt, Germany). The methanol used was of HPLC gradient grade from J.T. Baker (Deventer, The Netherlands) and the water used was from Millipore, Milli-Q grade. The buffer solutions were filtered through 0.45-μm filters (Kebo, Spånga, Sweden).

### 3.3. Columns

The achiral and high capacity column Kromasil KR100-3.5$C_{18}$ (150×4.6 mm; 3.5 μm) was obtained from Eka Chemicals (Bohus, Sweden). The Chiral-AGP column (100×4.0 mm; 5 μm), was obtained from ChromTech (Hägersten, Sweden).

### 3.4. Preparation of mobile phases

The mobile phase used for the Kromasil column was methanol–water (70:30), it was prepared by mixing 3500 ml methanol and 1500 ml water. The mobile phase used for the Chiral-AGP column was an acetate buffer of pH 6.0 with ionic strength of $I=0.050$ $M$ and 0.25% 2-propanol. The buffer solutions were prepared by mixing 1.00 $M$ sodium acetate and concentrated acetic acid (17.49 $M$). The volume of acetic acid and sodium acetate solutions required to achieve the desired pH were calculated using the Henderson–Hasselbach equation. The exact pH value was measured and no further adjustments were made. The 2-propanol was added to the buffer by first lifting out exactly 12.50 ml buffer from a filled 5000-ml glass volumetric flask and then adding exactly 12.50 ml 2-propanol. All mobile phases were degassed in an ultrasonic bath before use.

### 3.5. Procedures

#### 3.5.1. Measuring isotherms

Adsorption isotherm of the two steroids 11α-OH-PS and AD were determined using the frontal analysis method in the staircase mode [20]. The adsorption data for LM and DM on Chiral-AGP, used as input data for the simulations in this study, was measured by Götmar et al. [16] using the FA method.

#### 3.5.2. Diode array detection (DAD)

DAD made it possible to use five different wavelengths for UV detection, The UV signal was recorded at 245 nm, 320, 330, 350 and 360 nm for the Kromasil KR100 column system and 224 nm, 230, 254, 260 and 280 nm for the Chiral-AGP column system.

#### 3.5.3. Column parameters

System I: All chromatographic and thermodynamic parameters for system I, are presented in Table 2. For other experimental conditions and procedures, see Ref. [20].

System II: All chromatographic and thermodynamic parameters for system II, are presented in Table 2. For other experimental conditions and procedures, see Ref. [16]. However, another column was used in this study and that is why the phase ratio $F$ in Table 2 is different from that of Ref. [16].

#### 3.5.4. Non-linear regression

The best parameters of the Langmuir isotherm were calculated using a non-linear regression method, the Gauss–Newton algorithm with the Levenberg modification, as implemented in the software PCNONLIN 4.2 from Scientific Consulting (Apex, NC, USA). System I was best fitted by a Langmuir adsorption model, see Table 2 and Ref. [20]. System

Table 2
Chromatographic parameters for system I respective system II

| Solute | Type of site | $a$ | $b$ ($mM^{-1}$) | $q_s = a/b$ ($mM$) |
|---|---|---|---|---|
| System I | | | | |
| 11α-OH-PS | | 2.58 | 0.00543 | 475 |
| AD | | 3.29 | 0.00506 | 650 |
| System II | | | | |
| LM/DM | I | 1.58 | 0.107 | 14.8 |
| LM | II | 9.62 | 3.03 | 3.17 |
| DM | II | 13.6 | 4.69 | 2.89 |

System I: The steroids 11α-OH-PS and AD on Kromasil KR100-3.5$C_{18}$ (particle size: 3.5 μm; 150 mm×4.6 mm I.D.) with methanol–water (70:30) as mobile phase. The parameters in the simple Langmuir model below were determined by the frontal analysis method [20]: $q = ac/(1+bc)$, with, $F_m = 0.60$ ml/min; $t_0 = 2.37$ min; $F = 0.753$; $N = 3000$; UV = 350 nm; $T = 25.0$ °C.
System II: The enantiomers LM and DM on Chiral-AGP (particle size: 5.0 μm; 100 mm×4.0 mm I.D.) with acetate buffer, pH 6.0 ($I = 0.050$ $M$) and 0.25% 2-propanol as mobile phase. The parameters in the bi-Langmuir model below were determined by the frontal analysis method [16]: $q = a_I c/(1+b_I c) + a_{II} c/(1+b_{II} c)$, with, $F_m = 0.80$ ml/min; $t_0 = 1.17$ min; $F = 0.343$; $N = 1500$; UV = 224 or 254 nm; $T = 23.0$ °C.

II was best fitted by a bi-Langmuir model, see Table 2 and Ref. [16].

## 4. Results and discussion

In this study, two phenomena are studied, which are taking place for perturbation peaks at moderate to strong non-linearity of binary and racemic plateaus; (i) peculiar retention behaviour and (ii) peak vanishing.

Recently, the PM method was suggested for measuring competitive data in chiral LC and the theory for the binary case was developed [11–13]; however high-capacity preparative systems was used in the experimental verification and thus only moderately degrees of non-linearity was reached. The degree of non-linearity can be estimated from the value of the fractional surface coverage $\theta$ as calculated from the equation $\theta = bc/(1 + bc)$ [16] where $\theta$ is the fraction of a monolayer built on the surface when it is in equilibrium with a certain plateau concentration $c$. The coefficient $b$ is the energy of interaction. We suggest that the fractional surface coverage $\theta\% < 10$ is considered as weakly non-linear, $10 \leq \theta\% \leq 50$ as moderately non-linear and $\theta\% > 50$ as strongly non-linear conditions

### 4.1. Chromatographic systems

Two different chromatographic systems were used in order to cover the whole range of non-linear conditions of the racemic plateaus.

#### 4.1.1. System I

This system is a high-capacity system showing homogenous adsorption and high efficiency (see Table 2). It is based on the achiral column Kromasil KR100-3.5$C_{18}$ (150×4.6 mm; 3.5 μm) using as mobile phase methanol–water (70:30) and as solutes the steroids AD and 11α-OH-PS. The best thermodynamic coefficients of the Langmuir model were determined in another work [20] and are presented in Table 2. This system is perfect to serve as a model for a chiral high capacity system such as those recently studied with the PM method [11–13,21] since a homogenous adsorption model (Langmuir) is used and since the compounds AD and 11α-OH-PS has identical spectra.

#### 4.1.2. System II

This system is a low-capacity system showing heterogeneous adsorption and low efficiency, see Table 2, based on the chiral column Chiral-AGP (100×4.0 mm; 5 μm) consisting of $\alpha_1$-acid glycoprotein immobilised on porous silica. This is the most popular protein column today because of its unique ability to separate enantiomers of many different classes of chiral compounds [15]. The solutes used were LM and DM. The adsorption of the solutes on this protein is heterogeneous; the bi-Langmuir model fitted best to the adsorption and the parameters was presented in another work [16] and is listed in Table 2. The bi-Langmuir model consists of two sets of Langmuir terms at the right hand side of the equality sign. One of the Langmuir terms represents a high-density of the non-enantioselective interactions, so-called type I sites. The other term represents a fewer number of enantioselective interactions, so-called type II sites.

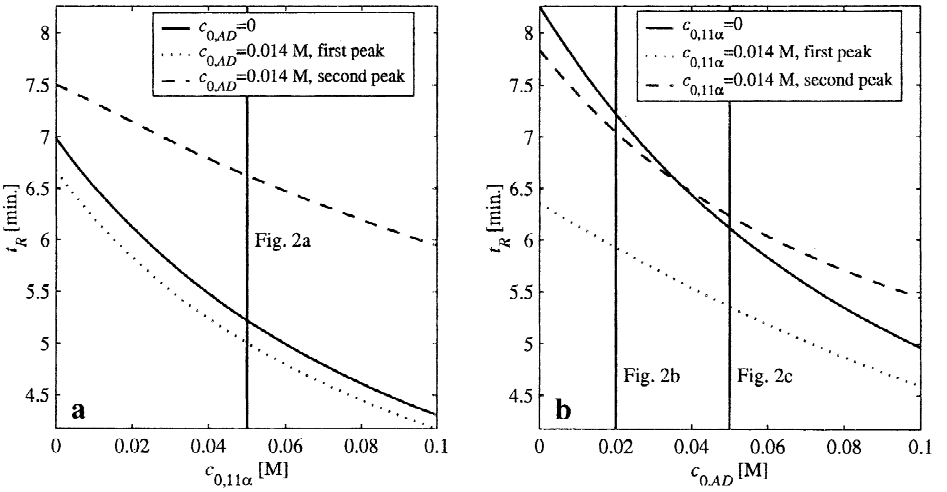


Fig. 1. Calculated retention times of single and binary perturbation peaks versus plateau concentrations as calculated from Eq. (8) for the parameters of Table 2, system I. (a) Retention times versus the plateau concentration $c_{0,11\alpha}$ of the less-retained component 11α-OH-PS with and without a constant plateau $c_{0,AD}$ of AD. (b) Retention times versus the plateau concentration $c_{0,AD}$ of the more-retained component AD with and without a constant plateau $c_{0,11\alpha}$ of 11α-OH-PS.

### *4.2. Peculiar retention behaviour*

Fig. 1a and b show calculated retention times of single and binary perturbation peaks, as a result of analytical size perturbations, versus plateau concentrations as calculated from the parameters for system I, Table 2. In Fig. 1a the retention times are plotted versus an increasing single plateau concentration of the less retained compound 11α-OH-PS (solid line). In the same figure there is also the retention times of the two perturbation peaks resulting from perturbation of the binary plateau consisting of an increasing plateau concentration of 11α-OH-PS and a constant concentration of AD, $c_{0,AD}$ 0.014 *M*. In Fig. 1b the retention times of the perturbation peak is plotted versus an increasing single plateau concentration of the more-retained compound AD as well as versus an increasing AD plateau concentration containing 0.014 *M* 11α-OH-PS. The retention time of the perturbation peaks decreases in all cases with increasing plateau concentration of the compound according to what is expected from the theory based on the Langmuir model. It must be noted that the perturbation peak on the single plateau (solid line in Fig. 1a) of the less retained 11α-OH-PS is always eluted between the two perturbation peaks of the corresponding binary plateau (see Fig. 1a) whereas the single plateau peak of the more retained AD is eluting after both binary perturbation peaks at low plateau levels and in between them at high levels (see Fig. 1b) with an intersection point at around $c_{0,AD}$ 0.037 (at $\theta\% = 15.8$). This latter retention behaviour which is in accordance with the Langmuir theory might be difficult to accept for the general chromatographer. A wrong conclusion of this ''peculiar'' retention behaviour would be that a retention reversal has been taking place. This is wrong because the two binary perturbation peaks can not be identified (see Section 2).

In Fig. 2a–c the conditions marked with lines in Fig. 1a and b is verified experimentally. Fig. 2a (i) shows the resulting chromatogram after perturbation of the single plateau of the less retained 11α-OH-PS at $c_{0,11\alpha}$ 0.050 *M* ($\theta\% = 21.4$) and its peak has $t_R = 5.22$ min. In Fig. 2a (ii) the plateau $c_{0,AD}$ 0.014 *M* is added on top of the 11α-OH-PS plateau and the first perturbation peak has $t_R = 5.02$ min. and the second one $t_R = 6.67$ min. These retention times shows excellent agreement with the calculated results in Fig. 1a (vertical line denoted Fig. 2a). The chromatograms in Fig. 2b and c provide the experimental verification of the situation when we have an increasing single and binary plateau concentration of the more-retained AD, cf. the two corresponding

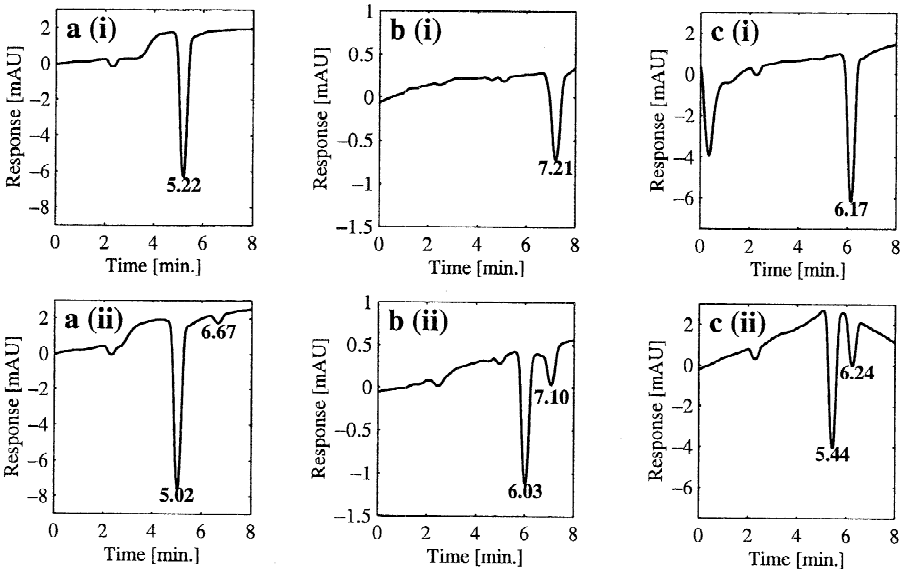


Fig. 2. Experimental chromatograms resulting from perturbation of selected (i) single and (ii) binary plateaus as predicted from Fig. 1a–b. The plateau concentrations are as follows: (a) (i) $c_{0,11\alpha}=0.050$ *M*, (ii) $c_{0,11\alpha}=0.050$ *M*, $c_{0,AD}=0.014$ *M*. (b) (i) $c_{0,AD}=0.020$ *M*, (ii) $c_{0,AD}=0.020$ *M*, $c_{0,11\alpha}=0.014$ *M*. (c) (i) $c_{0,AD}=0.050$ *M*, (ii) $c_{0,AD}=0.050$ *M*, $c_{0,11\alpha}=0.014$ *M*. The injection is 5 μl of pure mobile phase lacking both AD and 11α-OH-PS, i.e., $c_{s,11\alpha}=c_{s,AD}=0$. Experimental conditions: see Table 2, system I.

vertical lines in Fig. 1b. Fig. 2b (i) shows the resulting chromatogram after the perturbation of the single plateau $c_{0,AD}$ 0.020 *M* ($\theta\%=9.2$) and this perturbation peak has $t_R=7.21$ min. When $c_{0,11\alpha}$ 0.014 *M* is added on top of this plateau the first perturbation peak has $t_R=6.03$ min and the second one $t_R=7.10$ min, cf. Fig. 2b (ii). This situation corresponds to the first vertical line in Fig. 1b where the retention time of the single perturbation peak is higher than the retention times of both perturbation peaks in the binary plateau. Fig. 2c (i) shows the resulting chromatogram after perturbation of the single AD plateau at $c_{0,AD}$ 0.050 *M* ($\theta\%=20.2$). The single perturbation peak of AD has the retention time $t_R=6.17$ min which is in between the first and second perturbation peak at the corresponding binary plateau where $t_R=5.44$ min and $t_R=6.24$ min, respectively. This experimental situation corresponds to the second vertical line in Fig. 1b, showing excellent agreement with the calculated data.

### *4.3. Vanishing perturbation peaks in chiral LC*

When performing the PM method for determination of binary adsorption isotherm data, analytical-size injections of eluent lacking the plateau compounds are recommended at successively increasing or decreasing plateaus [11,21] resulting in two negative perturbation peaks for each plateau concentration [12]. However, this approach (i.e., analytical-size blank injections) works only as long as the racemic plateau is only in the weakly ($\theta\%<10$) to near-moderate non-linear regions and not at stronger surface coverages.

The experiments below will demonstrate this problem using system II, showing a heterogeneous adsorption with two types of sites (see Table 2). We begin with a low racemic plateau level; the concentration of each enantiomer, DM and LM, is 0.0125 m*M*. At this plateau the $\theta\%$ values for the type I sites were 0.1 and for the type $II_{LM}$ and type $II_{DM}$ sites 3.6 and 5.5, respectively. Thus, the type I sites were operated in the linear region and the type II sites in the weakly non-linear region. A perturbation was made on this binary plateau by injection a sample of 5 μl eluent lacking the plateau components, i.e., $c_{0,DM}=c_{0,LM}=0$. The resulting experimental chromatogram has two negative perturba-

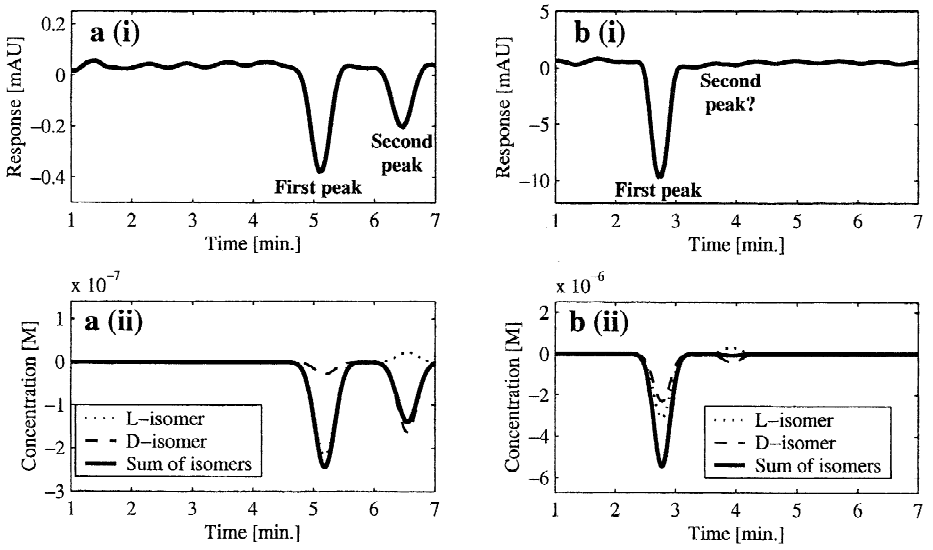


Fig. 3. Vanishing perturbation peaks in chiral LC at racemic plateaus at (a) weak and (b) moderate non-linear levels; (i) experimental chromatograms and (ii) simulated showing the sum and the individual concentration of the LM and DM isomers, respectively. (a) The plateau concentration is $c_{0,DM}=c_{0,LM}=0.0125$ m*M* and the injection is 5 μl of pure mobile phase lacking both LM and DM isomers, i.e., $c_{s,DM}=c_{s,LM}=0$. (b) The plateau concentration is $c_{0,DM}=c_{0,LM}=0.15$ m*M* and the injection is 5 μl of pure mobile phase lacking both LM and DM isomer, i.e., $c_{s,DM}=c_{s,LM}=0$. Experimental conditions: see Table 2, system II (UV=224 nm).

tion peaks, see Fig. 3a (i). Interestingly, the relative areas of the first and second peak are 63.9 and 36.1%, i.e., the area of the second peak is somewhat smaller than the area of the first. The explanation is given in the corresponding calculated chromatogram where the individual concentrations of the enantiomers are calculated together with their sum, see Fig. 3a (ii). The concentration of the less-retained LM isomer (dotted line) is deeply negative in the first perturbation peak and the more-retained DM isomer (dashed line) is deeply negative in the second perturbation peak. However, in the first perturbation peak there is also a slight negative deviation of the more-retained D isomer and in the second perturbation peak there is a slight positive deviation of the less-retained L isomer. Thus, the simulated sum of the LM and DM isomer concentrations (solid line) gives a larger relative area for the first perturbation peak than for the second one. The experimental chromatograms show an excellent agreement with the simulated ones, cf. Fig. 3a (i) and (ii).

However, as the racemic plateau concentration was increased the relative area of the second perturbation peak decreased continuously in the resulting experimental chromatograms. At the racemic plateau concentration of 0.15 m*M* of each enantiomer, the $\theta$% value of the type I site was 1.6 while that of type II sites were 31.3 for LM and 41.3 for DM. Thus, the degree of non-linearity of the type II sites were moderate and in the similar magnitude as the maximum plateaus as calculated from the homogenous surfaces studied previously [11,13]. After injection of a 5 μl blank injection on this racemic plateau the experimental chromatogram showed only one perturbation; the second one had vanished completely, see Fig. 3b (i). The corresponding simulation revealed that the individual isomer deviate in opposite directions, D isomer negative and L isomer positive, at the position of the second retention time and that they have almost equal magnitudes, see Fig. 3b (ii). Therefore, the sum-signal at the second retention time is more or less cancelled.

### *4.4. Prediction of optimal injection technique*

The problem of recognising the second perturbation peak in a racemic plateau is the main difficulty

for the use of the PM method in chiral LC. One empirical solution was found by systematic computer simulations; a sample was injected composed of only the plateau concentration of the less-retained enantiomer. This resulted in a chromatogram with two peaks; however, at further increased racemic plateau concentrations the second peak vanished again, in the general baseline noise.

However, an optimal approach was found on a firm theoretical basis, see Section 2.3. The situation when one perturbation peak vanishes, i.e., when the total peak area in the chromatogram becomes zero, was expressed in mathematical terms. It was concluded that any injection with the sample concentration $c_{s,1}=c_{0,1}-\mu$ and $c_{s,2}=c_{0,2}+\mu$ for some number $\mu$ chosen so that $c_{s,1}\geq 0$ and $c_{s,2}\geq 0$, will always yield two perturbation peaks with the same area but opposite signs, i.e., one positive and the other one negative, cf. Eq. (13). This optimal injection does not depend on the isotherm. One variant of the technique was actually predicted by one of the authors (J.L.) before predicted theoretically; thus we call it the ''Lindholm-technique''. The optimal injection in the case where both peaks have the same sign is expressed in Eq. (14), but this sample composition depends on the isotherm. Fig. 4a shows geometrically Eqs. (13) and (14) and based on the parameters of system II, Table 2 and the plateau concentration $c_{0,\mathrm{DM}}=c_{0,\mathrm{LM}}=0.050$ m*M*. At this moderately non-linear plateau the $\theta$% values are 0.53 of type I sites, 13.2 of type $\mathrm{II}_{\mathrm{LM}}$ sites and 19 of type $\mathrm{II}_{\mathrm{DM}}$ sites. More particularly, Fig. 4a shows the sample compositions for inducing vanishing (solid lines) or optimal (dotted lines) perturbation peaks on this plateau. Notice that this plot is only valid for the racemic plateau given by the centre coordinates, $c_{0,\mathrm{DM}}=c_{0,\mathrm{LM}}=0.050$ m*M*. Fig. 4b shows the situation where the plateau concentration is increased to $c_{0,\mathrm{DM}}=c_{0,\mathrm{LM}}=1.0$ m*M*. This is a strongly nonlinear racemic plateau and the relative surface coverages ($\theta$%) are 9.7 (type I), 75.2 (type $\mathrm{II}_{\mathrm{LM}}$) and 82.4 (type $\mathrm{II}_{\mathrm{DM}}$). In this case, the optimal injections and the injection which causes the less retained perturbation peak to vanish are very close, i.e., only small

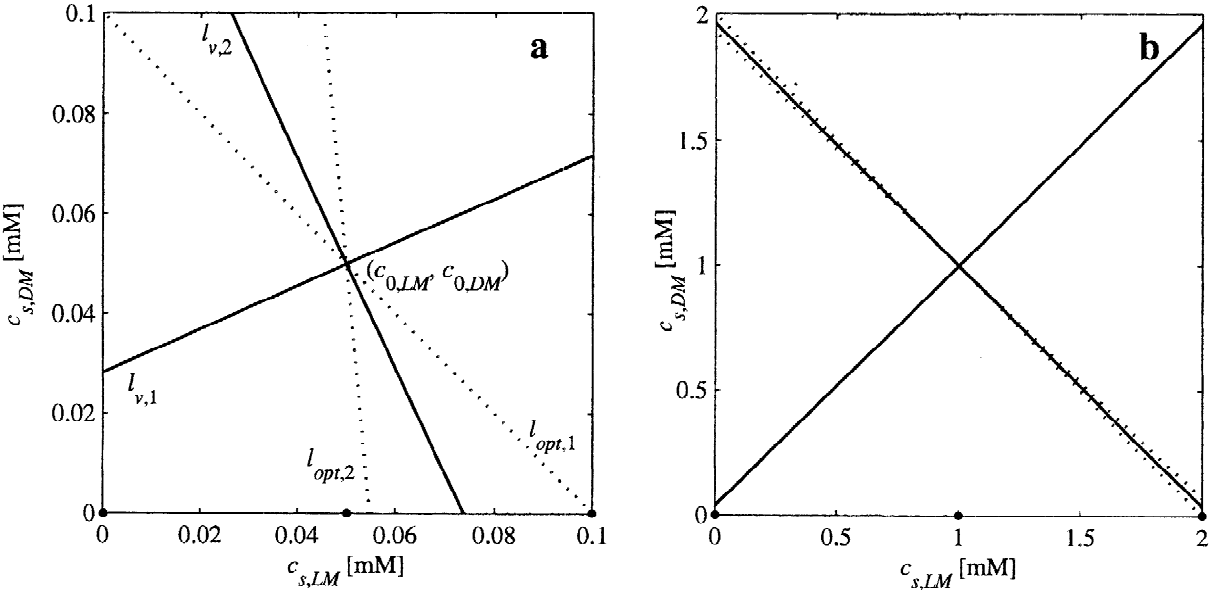


Fig. 4. (a) Figure showing calculated sample compositions for inducing vanishing (solid lines) or optimal (dashed lines) perturbation peaks on a moderately non-linear and racemic plateau of system II (see Table 2) when $c_{0,\mathrm{DM}}=c_{0,\mathrm{LM}}=0.05$ m*M*. Above $l_{\mathrm{v},1}$ is a line inducing the second peak to vanish, $l_{\mathrm{v},2}$ is a line inducing the first peak to vanish, $l_{\mathrm{opt},1}$ is a line inducing two peaks with the same area but different sign and $l_{\mathrm{opt},2}$ is a line inducing two peaks with the same area and sign. Notice that the lines inducing vanishing and optimal peaks are only valid for the specified plateau concentration. The three dots indicate the sample compositions injected in Fig. 6. (b) The same as (a) but the racemic plateau was strongly non-linear, $c_{0,\mathrm{DM}}=c_{0,\mathrm{LM}}=1$ m*M*. The three dots indicate the sample compositions injected in Fig. 7.

changes in the sample compositions are required to go from an optimal injection to an injection which causes one peak to disappear (cf. Fig. 4b). Notice that the slope of the line which gives sample compositions for the optimal injections, resulting in peaks with opposite sign, are the same in Fig. 4a and b, this is exactly in accordance with Eq. (13), i.e., the slope of this line does not depend on the plateau concentration. In addition, notice that the slope of all other lines changes, i.e., their slope depend on the plateau concentration as well as the isotherm.

### *4.5. Verification of optimal injection techniques*

Fig. 5a and b shows the relative areas of the less-retained and more-retained enantiomer peak, respectively, using different injection techniques on racemic plateaus of increasing concentrations as calculated for system II, Table 2. Using the blank injection technique, as suggested traditionally [11,13], the relative area of the first peak increases and are close to 100% at 0.4 m*M* of racemic plateau, i.e., $c_{0,\mathrm{DM}}=c_{0,\mathrm{LM}}=0.2$ m*M*, of course, the relative area of the second peak decreases towards 0% at the same rate. At this plateau when the second peak is completely vanished using the blank injection as perturbation method the plateau is only moderately non-linear (averaged $\theta$% for the type II sites is 43.1). Using the ''empirical approach'' it is possible to reach a somewhat higher racemic plateau level before the relative areas flattens out, in this case approximately at the racemic plateau level of 0.8 m*M*, i.e., $c_{0,\mathrm{DM}}=c_{0,\mathrm{LM}}=0.4$ m*M*. However, by using the optimal injection technique as predicted by Eq. (13), the relative area will constantly be 50% for both perturbation peaks independent of the racemic plateau concentration.

Fig. 6a–c show (i) experimental chromatograms and (ii) calculated ones at the moderately non-linear plateau $c_{0,\mathrm{DM}}=c_{0,\mathrm{LM}}=0.050$ m*M* (same binary plateau as in Fig. 4a) after the use of the various injection techniques suggested above on system II, Table 2. In Fig. 6a the perturbation was made by a blank injection; 5 μl of eluent lacking both LM and DM. The resulting experimental chromatogram shows a deep negative first peak and a small negative second one; the relative areas of the peaks are 87.7% and 12.3%, respectively. The individual concentrations for the enantiomers LM and DM as well as their sum are shown in the corresponding calculated chromatogram in Fig. 6a (ii). The calculated chromatogram revealed that the individual D enantiomer concentration has a somewhat deeper deviation at the second retention time as compared to the positive

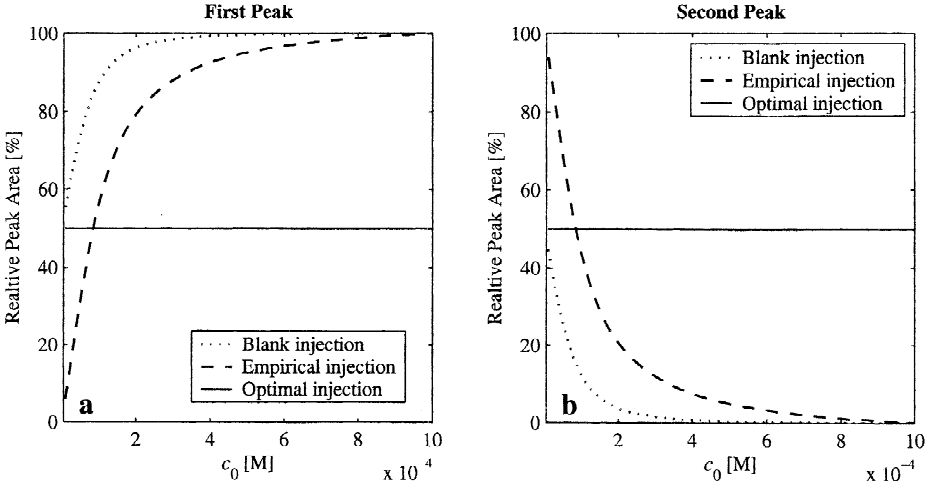


Fig. 5. Calculated relative area of perturbation peaks induced in three ways for system II, Table 2 on different binary plateaus were $c_{0,\mathrm{DM}}=c_{0,\mathrm{LM}}=c_0/2$. The blank injection technique is $c_{\mathrm{s,DM}}=c_{\mathrm{s,LM}}=0$, the empirical is $c_{\mathrm{s,DM}}=0$, $c_{\mathrm{s,LM}}=c_0/2$ and the optimal is $c_{\mathrm{s,DM}}=0$, $c_{\mathrm{s,LM}}=c_0$. (a) Relative area of the less retained perturbation peak. (b) Relative area of the more retained perturbation peak.

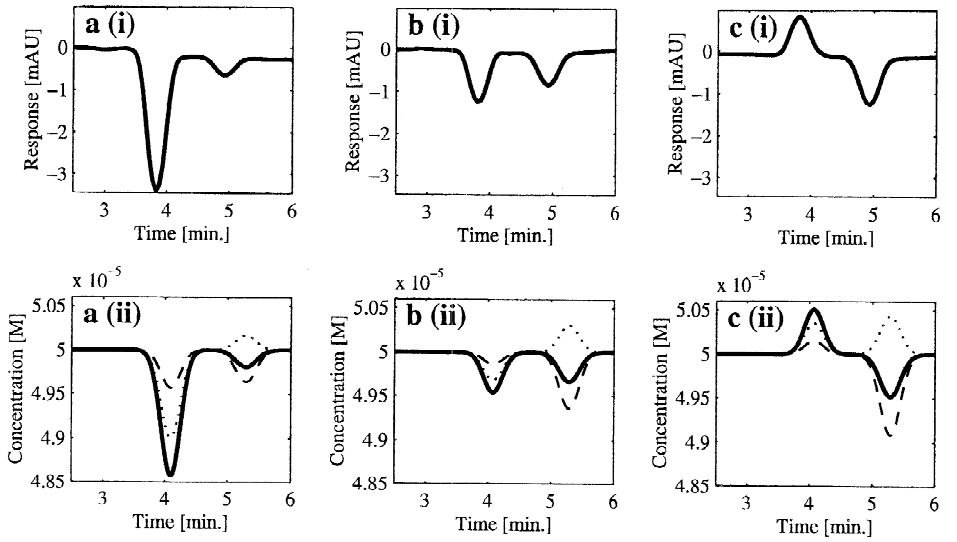


Fig. 6. Visualisation of both perturbation peaks with experimental verified (i) and calculated (ii) chromatograms after perturbation of a moderately nonlinear racemic plateau using the (a) blank (b) empirical and (c) optimal injection techniques, respectively. Dotted lines indicate the concentration of LM, dashed lines the concentration of DM and solid lines the total concentration or total response. The plateau concentrations of LM and DM are $c_{0,LM}$, $=c_{0,DM}=0.05$ m*M* and: (a) injection is 5 μl of eluent lacking both LM and DM, i.e., $c_{s,DM}=c_{s,LM}=0$. (b) Injection is 5 μl of eluent lacking only DM, i.e., $c_{s,DM}=0$, $c_{s,LM}=0.05$ m*M*. (c) Injection is 5 μl of eluent lacking DM and with 0.1 m*M* LM, i.e., $c_{s,DM}=0$, $c_{s,LM}=0.1$ m*M*. Experimental conditions: see Table 2, system II (UV=224 nm).

deviation of the L enantiomer at the same retention time. The relative calculated area of the first and second peak of the total sum-signal in this situation agrees very well with the experiment ones and can be read from Fig. 5a and b to 87.7% and 12.3%. In Fig. 6b the empirical injection technique was used by injecting a 5 μl of eluent lacking only DM. The resulting experimental chromatogram shows that the second peak is a negative peak and clearly discriminated from the baseline, see Fig. 6b (i). The relative areas of the first and second peak were 59.6 and 40.4%, respectively. The individual concentrations for the enantiomers LM and DM as well as their sum for this injection technique was calculated and presented in Fig. 6b (ii). The relative areas of the first and second peaks as read from Fig. 5a and b and was 56.5 and 43.4%, respectively, which agrees very well with the experimental situation. Even if the second perturbation peaks is more easily recognised by the empirical injection technique as compared to the blank injection there are two drawbacks. First, when the plateau level is close to linear the first perturbation peak will not be recognised since its sample concentration is its plateau level. This can be recognised in Fig. 5a where the relative area of the empirical approach (dashed line) goes towards zero at low plateau concentrations. The second drawback is that the second peak disappears again at a further increased racemic plateau, cf. Fig. 5b. The optimal injection technique according to Eq. (13) results in perturbation peaks that will always be of the same size but have opposite signs, the required sample composition is also illustrated by the line $l_{opt,1}$ in Fig. 4a. Practically this is a sample that, compared to the plateau concentration, is composed of a certain excess of one of the enantiomers and the same deficiency of the other enantiomer. In Fig. 6c we have (i) an experimental and (ii) a simulated chromatogram after the application of the optimal approach; in this case 5 μl of eluent containing 0.1 m*M* LM and lacking DM was injected. It can be seen that the relative areas are close to 50% in both the experimental and calculated chromatograms. The injection made above is just one possibility and any sample composition along the line $l_{opt,1}$ in Fig. 4a will do. The three sample compositions used in the

Fig. 6a–c is denoted by points at the *x*-axis of Fig. 4a.

### *4.6. Use of the optimal injection technique at strongly non-linear conditions*

In system II, Table 2, and in similar heterogeneous systems using protein chiral stationary phases (CSPs) for the separation of enantiomeric drugs, it is absolutely necessary to be able to reach plateau concentrations of 1 to 5 m*M* [16,18] corresponding to type II coverages, i.e., $\theta$% values, close to 100. If these concentrations are not reached the high capacity type I sites will not reach moderately non-linear conditions, and the error will be too large for the parameters of these type of sites [18]. We compared the different injection techniques on system II, Table 2 for the racemic plateau concentration of 2 m*M*, i.e., $c_{0,DM}=c_{0,LM}=1.0$ m*M*; this is the same strongly non-linear plateau as in Fig. 4b. Fig. 7a shows the resulting chromatogram with the blank injection (dotted line) and the empirical approach (dashed line), and none of the techniques made it possible to detect a second peak. This is in accordance with Fig. 5b predicting that the relative area of the second peak for also the empirical approach has reached 0% already at the racemic plateau concentration 0.8 m*M*, i.e., $c_{0,DM}=c_{0,LM}=0.4$ m*M*. Using the optimal injection technique, as suggested by Eq. (13), the second peak was visible also at this very high degree of non-linear racemic plateau, see Fig. 7b. The three sample compositions used in Fig. 7a and b is denoted by points at the *x*-axis of Fig. 4b.

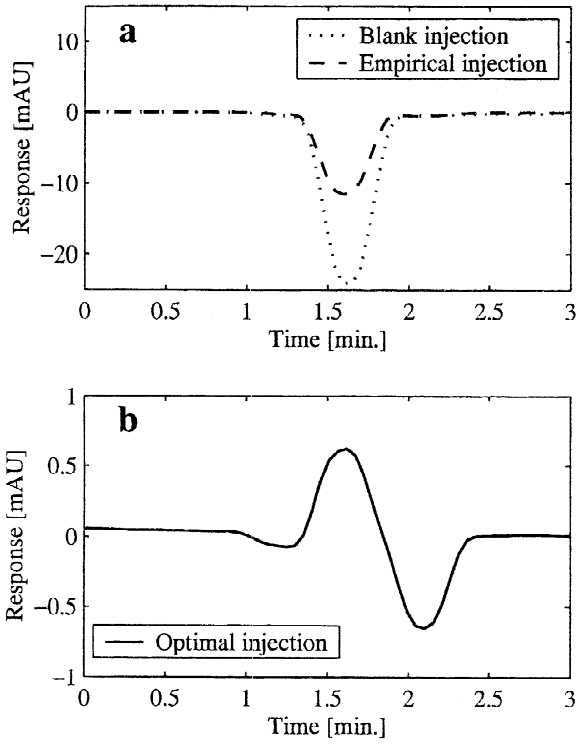


Fig. 7. Experimental chromatograms after perturbation of a strongly non-linear racemic plateau using the (a) blank and empirical and (c) the injection techniques in order to visualise both peaks. The plateau concentration is $c_{s,DM}=c_{s,LM}=1.00$ m*M* and: (a) blank injection is 20 μl of eluent lacking both LM and DM, i.e., $c_{s,DM}=c_{s,LM}=0$ and empirical injection is 20 μl of eluent lacking only DM, i.e., $c_{s,DM}=0$, $c_{s,LM}=1.00$ m*M*. (b) Optimal injection is 20 μl of eluent lacking DM and with 2 m*M* LM, i.e., $c_{s,DM}=0$, $c_{s,LM}=2.00$ m*M*. Experimental conditions: see Table 2, system II (UV=254 nm).

## 5. Conclusions

The theory for binary perturbation peaks in LC (e.g., racemic plateaus) was developed for both retention times and areas with focus on effects taking place during moderate ($10\leq\theta\%\leq50$) and strongly ($\theta\%>50$) degrees of non-linearity.

A peculiar retention behaviour was recognised and investigated; the single plateau peak of the more retained enantiomer is eluting after both binary perturbation peaks at low plateau levels and in between these peaks at high plateau levels. This phenomenon is not a retention reversal, since this interpenetration assumes that the two binary perturbation peaks can be identified, which is impossible from a theoretical standpoint.

A serious disadvantage with the ordinary perturbation approach is that the second perturbation peak vanishes already at moderate plateau concentrations. The strategy to solve the problem presented in this work is firmly supported by theory and has been verified experimentally during strongly non-linear conditions. Other strategies found empirically did not work out well, especially not under extremely non-linear conditions.

## Acknowledgements

The authors wish to thank AstraZeneca R&D (Mölndal, Sweden), Amersham Biosciences (Uppsala, Sweden) and The Swedish National Board for Industrial and Technical Development (NUTEK) for the financial support of this project.

## References

[1] I. Quiñones, C.M. Grill, L. Miller, G. Guiochon, J. Chromatogr. A 867 (2000) 1.
[2] F. Charton, R.M. Nicoud, J. Chromatogr. A 702 (1995) 97.
[3] M. Juza, M. Mazzotti, M. Morbidelli, TIBTECH March (2000) 18.
[4] G. Guiochon, G. Shirazi, A.M. Katti, Fundamentals of Preparative and Nonlinear Chromatography, Academic Press, Boston, MA, 1994.
[5] T. Fornstedt, G. Guiochon, Anal. Chem. 73 (2001) 608A.
[6] A. Tiselius, Ark. Kemi Mineral. Geol., 14B (1940) No. 22.
[7] J.M. Jacobson, J.H. Frenz, Cs. Horváth, Ind. Eng. Chem. Res. 26 (1987) 50.
[8] C.N. Reilley, G.P. Hildebrand, J.W. Ashley Jr., Anal. Chem. 34 (1962) 1198.
[9] F. Helfferich, D.L. Peterson, Science 142 (1963) 661.
[10] D. Tondeur, H. Kabir, L.A. Luo, J. Granger, Chem. Eng. Sci. 51 (1996) 3781.
[11] C. Heuer, E. Küsters, T. Plattner, A. Seidel-Morgenstern, J. Chromatogr. A 827 (1998) 175.
[12] C. Blümel, P. Hugo, A. Seidel-Morgenstern, J. Chromatogr. A 865 (1999) 51.
[13] P. Jandera, S. Buncekova, K. Mihlbachler, G. Guiochon, V. Backovska, J. Planeta, J. Chromatogr. A 925 (2001) 19.
[14] T. Fornstedt, presented at the 24th International Symposium on High Performance Liquid Phase Separations and Related Techniques, Seattle, WA, 24–30 June 2000, paper L0806..
[15] J. Hermansson, M.J. Eriksson, J. Liq. Chromatogr. 9 (1986) 621.
[16] G. Götmar, N.R. Albareda, T. Fornstedt, Anal. Chem. 74 (2002) 2950.
[17] T. Fornstedt, G. Götmar, M. Andersson, G. Guiochon, J. Am. Chem. Soc. 121 (1999) 1164.
[18] G. Götmar, pH.D. Thesis, Uppsala University, Uppsala, 2002. Acta Univ. Upsaliensis, No. 267 (2002).
[19] L.A. Luo, H. Kabir, S. Chanel, D. Tondeur, Chem. Eng. Sci. 55 (2000) 5613.
[20] J. Lindholm, P. Forssén, T. Fornstedt, manuscript in preparation.
[21] K. Mihlbachler, A. Kaczmarski, A. Seidel-Morgenstern, G. Guiochon, J. Chromatogr. A 955 (2002) 35.